

## CLUES ON THE REJUVENATION OF THE S0 GALAXY NGC 404 FROM THE CHEMICAL ABUNDANCE OF ITS OUTER DISK

FABIO BRESOLIN

Institute for Astronomy, 2680 Woodlawn Drive, Honolulu, HI 96822  
bresolin@ifa.hawaii.edu

## ABSTRACT

The oxygen abundance of the outer disk of the nearby S0 galaxy NGC 404, a prototypical early-type galaxy with extended star formation, has been derived from the analysis of H II region spectra. The high mean value found,  $12 + \log(\text{O}/\text{H}) = 8.6 \pm 0.1$ , equivalent to approximately 80% of the solar value, argues against both the previously proposed cold accretion and recent merger scenarios as viable mechanisms for the assembly of the star-forming gas. The combination of the present-day gas metallicity with the published star formation history of this galaxy favors a model in which the recent star forming activity represents the declining tail of the original one.

*Subject headings:* galaxies: abundances — galaxies: ISM — galaxies: elliptical and lenticular, cD — galaxies: evolution — galaxies: individual (NGC 404)

## 1. INTRODUCTION

Studies of the gaseous content of early-type (E/S0) galaxies (ETGs) have established that gas accretion and the presence of H I reservoirs are common features among these systems (Oosterloo et al. 2010; Davis et al. 2011; Thom et al. 2012). The presence of gas is often accompanied by low-level, recent (age < 1 Gyr) star formation, which is detected in a significant fraction (> 30%) of the ETGs observed in the far-UV by the Galaxy Evolution Explorer (GALEX, Martin et al. 2005) (Yi et al. 2005; Kaviraj et al. 2007). Several authors (e.g. Serra et al. 2008; Kaviraj et al. 2009; Cortese & Hughes 2009) have invoked the supply of external gas via galaxy merging or interactions in order to explain the star forming and gas content properties of ETGs, as well as the rejuvenation (Rampazzo et al. 2007) of these systems, that had the bulk of their star formation virtually completed early in their history.

Star formation in ETGs is often confined to their outskirts, in the form of extended UV-bright ring-like structures (Donovan et al. 2009; Thilker et al. 2010; Salim & Rich 2010; Moffett et al. 2012), resembling the outer star-forming disks identified in late-type galaxies (Thilker et al. 2007). Despite their prominence in far-UV GALEX images of nearby ETGs, these rings account for only a few percent of the total stellar mass of the host galaxies (Marino et al. 2011).

In a recent study of 29 S0 galaxies at redshift  $z \sim 0.1$  Salim et al. (2012) critically reviewed the mechanisms that can generate spatially extended star formation in ETGs. Cold, smooth gas accretion from the intergalactic medium (IGM), as predicted by cosmological hydrodynamic simulations (e.g. Kereš & Hernquist 2009), was identified, based on qualitative optical/UV galaxy morphology, as the likely mechanism for rejuvenating the star formation activity in about half of their sample. The supply of gas from minor mergers and the fading of the original star formation (not requiring external gas sources) could explain the remaining cases. These conclusions have been strengthened in a related work by Fang et al. (2012), who included 670 extended star formation ETG candidates in their quantitative analysis of UV-optical colors. Thus, ETGs with extended star formation probably constitute a heterogeneous class, composed both by systems with declining star formation and others experiencing rejuvenation following gas accretion.

The nearest S0 galaxy, NGC 404 ( $D = 3.05$  Mpc, Dalcanton et al. 2009) has been identified by Thilker et al. (2010) as the host of recent star formation in its nearly face-on outer disk. UV-emitting young star clusters reside within an H I ring, extending between 1.5 and 6.5 kpc ( $1 - 4 R_{25}$ ) from the galactic center. The relatively small distance to NGC 404 and its isolation (Karachentsev et al. 2002) make this galaxy an ideal site where to explore the processes regulating the evolution of an ETG with extended star formation. Following the suggestion by del Río et al. (2004) that a merger with a dwarf galaxy supplied NGC 404 with fresh gas in the past Gyr, Thilker et al. (2010) argued that this lenticular galaxy is an example of a rejuvenated ETG, currently shifting from the red sequence of the bimodal optical color distribution of galaxies back into the green valley. This paper offers an alternative view, providing constraints on the nature of the extended star formation in NGC 404 from a chemical abundance analysis of H II regions lying in its outer disk.

## 2. OBSERVATIONS AND DATA REDUCTION

Observations of H II region candidates in the outer disk of NGC 404 were obtained with the Gemini Multi-Object Spectrograph (GMOS, Hook et al. 2004) at the Gemini North telescope. The targets were selected from H $\alpha$  narrow-band images of two  $5'.5 \times 5'.5$  GMOS fields in the outer, star-forming disk of the galaxy, approximately  $3'.9$  (3.4 kpc) E and  $4'.6$  (4.1 kpc) N of the center, respectively. Spectra were acquired on September 18, 2012, under  $0''.5$  FWHM seeing conditions, using two multi-object masks, one per field, containing  $1''.5$ -wide slits. Three 1800 s exposures were secured for each field using the B600 grating, providing spectra covering the  $\sim 4700$ - $7500$  Å wavelength range (the coverage depending on the spatial distribution of the targets), at a spectral resolution of  $6$  Å for nebulae filling the slit ( $3.5$  Å for six spatially unresolved objects).

IRAF<sup>1</sup> routines in the `gemini/gmos` package were used for electronic bias subtraction, flat field correction, wavelength calibration, and coaddition of the raw data frames. The spec-

<sup>1</sup> IRAF is distributed by the National Optical Astronomy Observatories, which are operated by the Association of Universities for Research in Astronomy, Inc., under cooperative agreement with the National Science Foundation.

TABLE 1  
H II region sample: coordinates and line ratios

ID	R.A. (J2000.0)	DEC (J2000.0)	$R$ (arcsec)	$R/R_{25}$	[O III] $\lambda$ 5007/H $\beta$	[N II] $\lambda$ 6583/H $\alpha$	[S II] $\lambda$ 6717,31/H $\alpha$	Comments
1	01 09 18.65	35 41 57.5	124	1.18	< 0.30	0.24	0.31	
2	01 09 18.94	35 42 14.9	111	1.06	7.87	0.04	< 0.02	PN candidate
3	01 09 08.62	35 43 08.2	224	2.14	...	0.20	0.18	
4	01 09 14.43	35 43 44.3	158	1.51	< 0.36	0.23	0.28	
5	01 09 14.21	35 43 50.7	162	1.55	4.87	0.42	0.91	SNR candidate
6	01 09 13.27	35 44 27.8	187	1.78	0.94	0.22	0.24	
7	01 09 19.48	35 45 10.8	157	1.49	1.20	0.21	0.17	
8	01 09 15.58	35 45 37.7	208	1.98	< 0.48	0.15	< 0.07	unresolved
9	01 09 16.24	35 46 41.7	256	2.44	0.15	0.23	0.19	
10	01 09 27.52	35 47 35.0	275	2.62	...	0.29	0.13	unresolved
11	01 09 27.52	35 47 35.0	275	2.62	...	0.20	0.33	unresolved
12	01 09 26.73	35 47 37.9	278	2.64	...	0.24	0.28	
13	01 09 40.57	35 47 55.2	339	3.23	...	0.21	0.14	unresolved
14	01 09 41.18	35 48 01.0	348	3.31	3.10	0.10	0.09	
15	01 09 39.84	35 48 30.5	367	3.50	0.15	0.17	0.22	
16	01 09 19.22	35 48 41.9	355	3.38	0.56	0.17	0.22	
17	01 09 22.06	35 48 43.8	350	3.33	< 0.28	0.21	0.26	
18	01 09 38.82	35 48 44.8	375	3.57	0.52	0.22	0.17	unresolved
19	01 09 26.25	35 49 22.9	385	3.66	< 0.43	0.21	0.27	

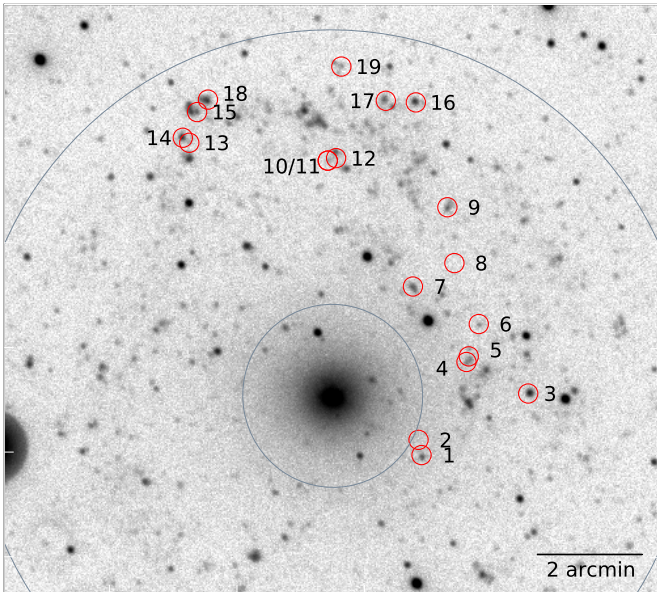


FIG. 1.— Identification of the targets on a near-UV GALEX image of NGC 404 (N at top, E on the left). The circles, drawn at radii  $R_{25}$  and  $4R_{25}$ , represent the approximate inner and outer boundaries of the star forming ring.

tra were not flux calibrated. This has virtually no effect on the analysis presented here, given the proximity in wavelength between the emission lines used to construct the nebular diagnostics. Two of the targets were found to be background emission-line galaxies, and were removed from the analysis. The final sample comprises 19 objects in an annulus between  $R_{25}$  and  $4R_{25}$  (hereafter referred to as the star-forming ring) of NGC 404. Their location is indicated in Fig. 1 (#10 and #11 are targets included in the same slit). Celestial coordinates are summarized in Table 1, together with galactocentric distances (in arcsec and in units of the isophotal radius  $R_{25} = 1''.75$ ), de-projected adopting the geometrical parameters from del R o et al. (2004).

### 3. CHEMICAL ABUNDANCE ANALYSIS

The emission lines covered in the observed spectral range include H $\alpha$ , [N II]  $\lambda$ 6583 and [S II]  $\lambda$ 6717, 6731 (the latter remained undetected in #2 and #8). For 14 targets the H $\beta$  and [O III]  $\lambda$ 5007 lines were also accessible. Table 1 reports the values (or upper limits) of the line ratios [O III]  $\lambda$ 5007/H $\beta$ , [N II]  $\lambda$ 6583/H $\alpha$  and [S II]  $\lambda$ 6717, 6731/H $\alpha$ , which are virtually independent of flux calibration and reddening corrections, given the small separation in wavelength of the lines involved.

Fig. 2 illustrates the excitation properties of the targets, showing their location in the [N II]/H $\alpha$  vs. [O III]/H $\beta$  and [S II]/H $\alpha$  vs. [N II]/H $\alpha$  diagrams. Three objects stand out as peculiar based on their line ratios: #2 and #8, classified as candidate planetary nebulae (consistent with the point-source appearance and the lack of a continuum), and #5 (a 58 pc-diameter ring identified as a supernova remnant). The rest of the sample is composed of bona fide H II regions, whose chemical analysis can be carried out using standard diagnostics.

The diagrams in Fig. 2 include curves representing H II region models from Dopita et al. (2006), calculated for ionizing cluster ages between 0.1 and 4 Myr, and different metallicities (0.2, 0.4, 1.0 and  $2.0 \times Z_{\odot}$ ). The parameter  $\mathcal{R} \propto M_{cl}/P_0$  (the ratio between cluster mass and pressure of the interstellar medium) is also varied between  $\log \mathcal{R} = -2$  (solid lines) and  $\log \mathcal{R} = 0$  (dashed lines), although this has only a secondary effect on the interpretation of the diagrams. According to these models, the bulk of the H II region sample has a metallicity slightly below solar. Since the model curves in the [N II]/H $\alpha$  vs. [O III]/H $\beta$  diagram become virtually vertical after a cluster age of 3 Myr, the same conclusion can also be drawn for the 5 objects having only an upper limit for the [O III]/H $\beta$  ratio.

In order to quantify the radial distribution of the nebular metallicities the abundance diagnostic  $N2 = \log([N II] \lambda 6583/H\alpha)$  was adopted, using the calibrations provided by Pettini & Pagel (2004, = PP04) and Denicol o et al. (2002, = D02). The resulting O/H abundances are presented in Fig. 3, using solid (PP04) and open (D02) circles. While most sources share a similar O/H ratio, #14 (identified in the figure) displays a significantly lower abundance. This object has the

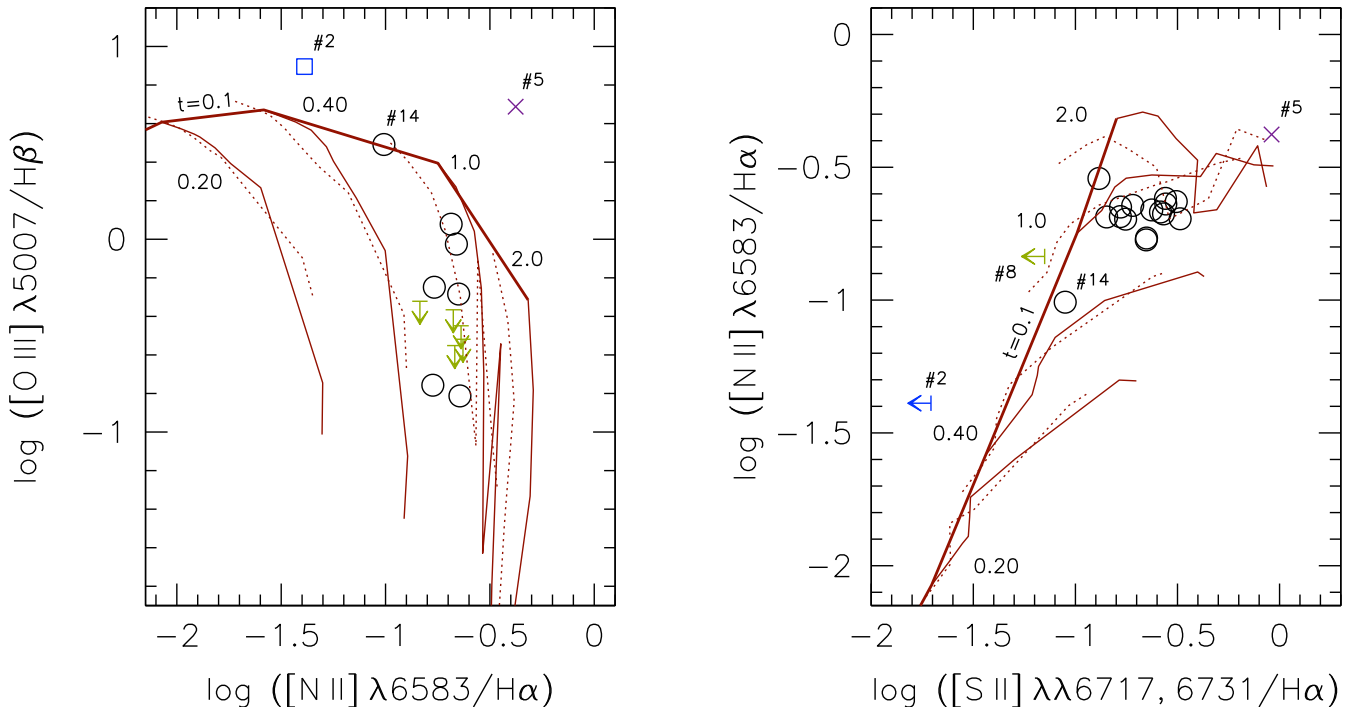


FIG. 2.— Excitation diagrams:  $[\text{N II}]/\text{H}\alpha$  vs.  $[\text{O III}]/\text{H}\beta$  (left) and  $[\text{S II}]/\text{H}\alpha$  vs.  $[\text{N II}]/\text{H}\alpha$  (right). Open circles: measured flux ratios. The candidate planetary nebulae (#2, #8) and supernova remnant (#5) are identified. The arrows represent upper limits. The curves show theoretical models from Dopita et al. (2006) calculated for ages 0.1–4 Myr, metallicities 0.2, 0.4, 1.0,  $2.0 \times Z_{\odot}$ ,  $\log \mathcal{R} = -2$  (solid lines) and  $\log \mathcal{R} = 0$  (dotted lines).

largest  $\text{H}\alpha$  equivalent width ( $950 \text{ \AA}$ ) in the sample, indicating a very young nebula, which is supported by the models in Fig. 2 (point lying on the 0.1 Myr curve). The position of #14 in relation to the model curves also shows that, despite the low  $[\text{N II}]/\text{H}\alpha$  ratio (which leads to the anomalous low O/H ratio using the strong-line abundance diagnostics), its metallicity is in fact comparable to that of the rest of the sample.

A least-squares fit to the data points (excluding the outlier #14) using the PP04 calibration yields a radial galactocentric gradient  $12 + \log(\text{O}/\text{H}) = 8.55 (\pm 0.03) - 0.014 (\pm 0.010) R/R_{25}$ . The (virtually flat) gradient's slope is unchanged using the D02 calibration, and can be expressed as  $d(\text{O}/\text{H})/dR = -0.009 (\pm 0.007) \text{ dex kpc}^{-1}$ . The mean abundance values are  $\langle 12 + \log(\text{O}/\text{H}) \rangle_{\text{PP04}} = 8.52 (\pm 0.03)$  and  $\langle 12 + \log(\text{O}/\text{H}) \rangle_{\text{D02}} = 8.63 (\pm 0.04)$ , respectively. An additional indication of the gas metallicity is provided by the  $\text{O3N2} = \{\log([\text{O III}] \lambda 5007/\text{H}\beta) - \text{N2}\}$  diagnostic (PP04) based on  $[\text{O III}] \lambda 5007$  detections (triangles in Fig. 3, mean  $12 + \log(\text{O}/\text{H}) = 8.65$ ) and upper limits (arrows). Systematic offsets between different calibrations are well known to exist (Kewley & Ellison 2008), and while their discussion is beyond the scope of this paper, it is important to point out for the following discussion that the N2 diagnostic, together with the *direct* method, tends to yield lower O/H ratios compared to alternative strong-line abundance determination methods (Bresolin et al. 2009a). In summary, the diagnostics considered here indicate that the oxygen abundance in the outer disk of NGC 404 is essentially constant, and I adopt a representative mean value  $12 + \log(\text{O}/\text{H}) = 8.6 \pm 0.1$ , equivalent to  $\sim 0.8 \times$  the solar value (Asplund et al. 2009). This result is consistent with the information provided by the photoionization models shown in Fig. 2.

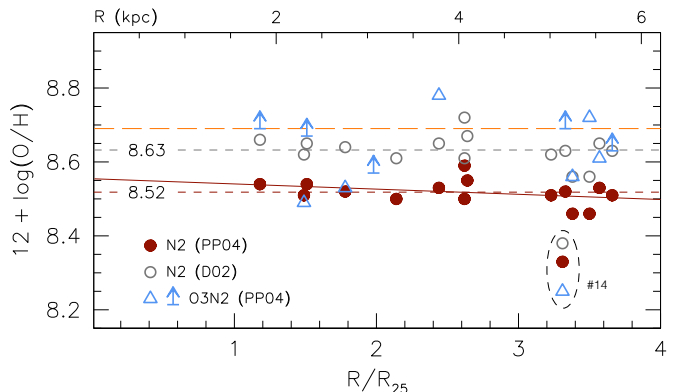


FIG. 3.— Radial distribution of the O/H abundance ratio obtained from the N2 diagnostic, using the calibrations of Pettini & Pagel (2004, =PP04) and Denicoló et al. (2002, =D02). The full line represents a least-squares fit to the data points measured with the PP04 calibration. The dashed lines show the mean values (indicated) of the O/H ratio resulting from the two calibrations. Triangles and arrows correspond to the abundances measured from the O3N2 diagnostic based on  $[\text{O III}] \lambda 5007$  detections and upper limits, respectively. The solar O/H value is indicated by the upper dashed line.

#### 4. DISCUSSION

The star formation history of NGC 404 has been recently investigated by Williams et al. (2010) from theoretical fits to the color-magnitude diagrams (CMDs) of the stellar populations in three WFPC2 fields observed with the *Hubble Space Telescope*. These fields cover the galactocentric distance range  $0.61 - 2.55 R_{25}$ , overlapping with the range spanned by the H II regions observed in this work ( $1.06 - 3.66 R_{25}$ ). The CMD analysis indicates that the majority (70%) of the stars in the disk (even in the outer star forming ring) formed earlier than 10 Gyr ago (90% formed by the end of the following

2 Gyr). The star formation rate (SFR) surface density declined from  $\sim 6.8 \times 10^{-3} M_{\odot} \text{ yr}^{-1} \text{ kpc}^{-2}$  early in the history of the galaxy to a negligibly small value ( $\lesssim 10^{-9} M_{\odot} \text{ yr}^{-1} \text{ kpc}^{-2}$ ) approximately 0.9 Gyr ago, when the gas surface density was extremely small ( $\sim 0.02 M_{\odot} \text{ pc}^{-2}$ ). The CMD fitting suggests that in the recent past ( $\sim 500$  Myr ago) the star formation activity resumed, with an estimated SFR density of  $2 \times 10^{-4} M_{\odot} \text{ yr}^{-1} \text{ kpc}^{-2}$  in the time interval between 0.5 and 0.2 Gyr ago (Williams et al. 2010, Fig. 14). This is about one order of magnitude higher than the current value estimated from the far-UV emission of the star-forming ring (Thilker et al. 2010). Williams et al. (2010) speculated that the increase in star formation activity was possibly triggered by the merger postulated by del Río et al. (2004), who studied with 21 cm observations the morphology and kinematics of the  $1.5 \times 10^8 M_{\odot}$  H I outer disk. del Río et al. (2004) identified the source of this gas with a merging dwarf galaxy about 0.5-1 Gyr ago, lending credibility to the rejuvenation scenario to explain the recent star formation in NGC 404.

Is this picture consistent with the chemical abundance analysis carried out in Sect. 3? It is worth comparing first the present-day gas metallicity with the stellar metallicity in the disk, as inferred by Williams et al. (2010) from the CMD modeling. As mentioned earlier, most of the galaxy's gas converted into stars very early on: the typical stellar age in NGC 404 is 12 Gyr, with a fitted metallicity  $[M/H] = -0.75 \pm 0.37$ . The declining star formation activity caused a progressive metal enrichment of the galaxy. The errors in  $[M/H]$  given by Williams et al. (2010) become too large ( $> 1$  dex) at recent times ( $< 200$  Myr ago) to offer a meaningful comparison with the H II region chemical abundances, but these authors estimated a stellar metallicity  $[M/H] = -0.38 \pm 0.35$  about 750 Myr ago. This is consistent with the value  $[M/H] \simeq -0.4$  measured by Seth et al. (2010) from spectra of the NGC 404 bulge (representative age: 5 Gyr). These results suggest that a chemical abundance comparable to the one obtained for the outer ring H II regions,  $[O/H] \simeq -0.1 \pm 0.1$ , was likely reached in the disk of this galaxy at least 1 Gyr ago (before the postulated merger), considering that for typical S0 galaxies  $[\alpha/\text{Fe}] \simeq 0.3$  (Sil'chenko et al. 2012; the H II regions provide a determination of the O/H ratio, while the stellar M/H given above is assumed to be representative of the Fe/H ratio).

If the general description of the star formation history of NGC 404 outlined by Williams et al. (2010) is broadly correct, the significant chemical enrichment measured for the outer disk H II regions argues against a gas-rich dwarf galaxy as the main source of fuel responsible for the re-ignition of the star formation, as proposed by del Río et al. (2004) and Thilker et al. (2010). From the stellar mass of NGC 404 measured by Thilker et al. (2010), and assuming a mass merger ratio of 1:3 (the maximum ratio commonly adopted to distinguish between major and minor mergers), the stellar mass of the merging dwarf would be  $1.5 \times 10^8 M_{\odot}$ . According to the mass-metallicity relation observed in the local universe (Berg et al. 2012) a galaxy with this mass has an oxygen abundance  $12 + \log(O/H) \simeq 7.98 \pm 0.15$ .<sup>2</sup>

Allowing for star formation over a period of 0.3 Gyr at a rate of  $2 \times 10^{-4} M_{\odot} \text{ yr}^{-1} \text{ kpc}^{-2}$  (following Williams et al. 2010), considering an observed H I surface density in the star-forming ring  $\Sigma_{\text{HI}} = 1 M_{\odot} \text{ pc}^{-2}$  (del Río et al. 2004) and with

an initial oxygen abundance  $12 + \log(O/H) \simeq 7.98$ , I estimate a final abundance of only  $12 + \log(O/H) \simeq 8.16$ , considering an oxygen yield of 0.01 (see Eq. 1 in Bresolin et al. 2012). Even if we double this period of enhanced star formation to 0.6 Gyr (which is excluded by the star formation history of the galaxy presented by Williams et al. 2010), the present-day oxygen abundance would be  $12 + \log(O/H) \simeq 8.30$ , still 0.3 dex below the observed value. Even considering the uncertainty in the estimated mass of the merging dwarf, the scatter in the mass-metallicity relation and the uncertainty in the nebular O/H resulting from the use of the N2 diagnostic (Pérez-Montero & Contini 2009), it appears difficult to explain the chemical enrichment of the outer disk of NGC 404 with the proposed dwarf galaxy merger.

The relatively high nebular metallicity of the star-forming ring of NGC 404 also rules out (metal-poor) primordial IGM gas accretion as the primary source of its star-forming gas (which has been proposed as a viable mechanism for the formation of metal-poor galactic ring structures, e.g. by Finkelman et al. 2011 and Spavone et al. 2010). On the other hand, a near-solar metallicity would be expected if the bulk of the gas has been part of the galaxy since its early history, and has been progressively chemically enriched by the star formation that has occurred in the disk (in agreement with the declining star formation scenario discussed by Salim et al. 2012 and Fang et al. 2012), although this possibility was deemed unlikely by del Río et al. (2004), based on the warped nature of the H I structure, which suggests that the gas has been acquired recently, and on critical gas density arguments (invalidated by the GALEX detection of recent star formation). It is conceivable that a perturbing event (minor/dry merger) took place in the recent past, that revitalized the star formation activity, but it is unlikely, based on the reconstructed star formation history, that such an event was responsible for the accretion of the gas, because of the incompatible chemical composition. It is also possible to argue in favor of an enriched accretion mechanism, as proposed in recent studies of the chemical abundances of the outer disks of spiral galaxies (Bresolin et al. 2009b, 2012; but I also note that these structures are  $3 \times$  larger than the outer disk of NGC 404), where the gas, chemically enriched by stellar processes in the disk, is subject to a wind-recycling mechanism, and inflows back into the disk (Davé et al. 2011; Martin et al. 2012).

In conclusion, this work shows that the chemical abundance analysis of the ionized gas provides crucial constraints on the origin of the outer star forming rings and potential rejuvenation events observed in ETGs. In particular, two of the main scenarios proposed, cold accretion and minor merger, are ruled out in the case of NGC 404 by the high nebular metallicity observed. Future work will test whether the declining star formation scenario provides a better fit to the present-day gas metallicity of additional ETGs.

FB gratefully acknowledges the support from the National Science Foundation grant AST-1008798, and thanks the anonymous referee for constructive comments.

<sup>2</sup> The gas metallicities obtained from the N2 method used here are on the same absolute scale as the *direct* metallicities measured by Berg et al. (2012).

## REFERENCES

- Asplund, M., Grevesse, N., Sauval, A. J., & Scott, P. 2009, *ARA&A*, 47, 481
- Berg, D. A., Skillman, E. D., Marble, A. R., et al. 2012, *ApJ*, 754, 98
- Bresolin, F., Gieren, W., Kudritzki, R., et al. 2009a, *ApJ*, 700, 309
- Bresolin, F., Kennicutt, R. C., & Ryan-Weber, E. 2012, *ApJ*, 750, 122
- Bresolin, F., Ryan-Weber, E., Kennicutt, R. C., & Goddard, Q. 2009b, *ApJ*, 695, 580
- Cortese, L., & Hughes, T. M. 2009, *MNRAS*, 400, 1225
- Dalcanton, J. J., Williams, B. F., Seth, A. C., et al. 2009, *ApJS*, 183, 67
- Davé, R., Finlator, K., & Oppenheimer, B. D. 2011, *MNRAS*, 415, 1158
- Davis, T. A., Alatalo, K., Sarzi, M., et al. 2011, *MNRAS*, 417, 882
- del Río, M. S., Brinks, E., & Cepa, J. 2004, *AJ*, 128, 89
- Denicoló, G., Terlevich, R., & Terlevich, E. 2002, *MNRAS*, 330, 69
- Donovan, J. L., Serra, P., van Gorkom, J. H., et al. 2009, *AJ*, 137, 5037
- Dopita, M. A., Fischera, J., Sutherland, R. S., et al. 2006, *ApJS*, 167, 177
- Fang, J. J., Faber, S. M., Salim, S., Graves, G. J., & Rich, R. M. 2012, *ApJ*, 761, 23
- Finkelman, I., Moiseev, A., Brosch, N., & Katkov, I. 2011, *MNRAS*, 418, 1834
- Hook, I. M., Jørgensen, I., Allington-Smith, J. R., et al. 2004, *PASP*, 116, 425
- Karachentsev, I. D., Sharina, M. E., Makarov, D. I., et al. 2002, *A&A*, 389, 812
- Kaviraj, S., Peirani, S., Khochfar, S., Silk, J., & Kay, S. 2009, *MNRAS*, 394, 1713
- Kaviraj, S., Schawinski, K., Devriendt, J. E. G., et al. 2007, *ApJS*, 173, 619
- Kereš, D., & Hernquist, L. 2009, *ApJ*, 700, L1
- Kewley, L. J., & Ellison, S. L. 2008, *ApJ*, 681, 1183
- Marino, A., Bianchi, L., Rampazzo, R., et al. 2011, *ApJ*, 736, 154
- Martin, C. L., Shapley, A. E., Coil, A. L., et al. 2012, *ApJ*, 760, 127
- Martin, D. C., Fanson, J., Schiminovich, D., et al. 2005, *ApJ*, 619, L1
- Moffett, A. J., Kannappan, S. J., Baker, A. J., & Laine, S. 2012, *ApJ*, 745, 34
- Oosterloo, T., Morganti, R., Crocker, A., et al. 2010, *MNRAS*, 409, 500
- Pérez-Montero, E., & Contini, T. 2009, *MNRAS*, 398, 949
- Pettini, M., & Pagel, B. E. J. 2004, *MNRAS*, 348, L59
- Rampazzo, R., Marino, A., Tantaló, R., et al. 2007, *MNRAS*, 381, 245
- Salim, S., Fang, J. J., Rich, R. M., Faber, S. M., & Thilker, D. A. 2012, *ApJ*, 755, 105
- Salim, S., & Rich, R. M. 2010, *ApJ*, 714, L290
- Serra, P., Trager, S. C., Oosterloo, T. A., & Morganti, R. 2008, *A&A*, 483, 57
- Seth, A. C., Cappellari, M., Neumayer, N., et al. 2010, *ApJ*, 714, 713
- Sil'chenko, O. K., Proshina, I. S., Shulga, A. P., & Koposov, S. E. 2012, *MNRAS*, 427, 790
- Spavone, M., Iodice, E., Arnaboldi, M., et al. 2010, *ApJ*, 714, 1081
- Thilker, D. A., Bianchi, L., Meurer, G., et al. 2007, *ApJS*, 173, 538
- Thilker, D. A., Bianchi, L., Schiminovich, D., et al. 2010, *ApJ*, 714, L171
- Thom, C., Tumlinson, J., Werk, J. K., et al. 2012, *ApJ*, 758, L41
- Williams, B. F., Dalcanton, J. J., Gilbert, K. M., et al. 2010, *ApJ*, 716, 71
- Yi, S. K., Yoon, S.-J., Kaviraj, S., et al. 2005, *ApJ*, 619, L111